

Thermodynamically stable lithium silicides and germanides from density-functional theory calculations

Andrew J. Morris*,¹ C. P. Grey,² and Chris J. Pickard³

¹*Theory of Condensed Matter Group, Cavendish Laboratory, University of Cambridge, J. J. Thomson Avenue, Cambridge CB3 0HE, United Kingdom*

²*Department of Chemistry, University of Cambridge, Lensfield Road, Cambridge CB2 1EW, United Kingdom*

³*Department of Physics and Astronomy, University College London, Gower St, London WC1E 6BT, United Kingdom*

(Dated: February 26, 2014)

High-throughput density-functional-theory (DFT) calculations have been performed on the Li-Si and Li-Ge systems. Lithiated Si and Ge, including their metastable phases, play an important technological rôle as Li-ion battery (LIB) anodes. The calculations comprise structural optimisations on crystal structures obtained by swapping atomic species to Li-Si and Li-Ge from the X-Y structures in the International Crystal Structure Database, where $X=\{\text{Li,Na,K,Rb,Cs}\}$ and $Y=\{\text{Si,Ge,Sn,Pb}\}$. To complement this at various Li-Si and Li-Ge stoichiometries, *ab initio* random structure searching (AIRSS) was also performed. Between the ground-state stoichiometries, including the recently found $\text{Li}_{17}\text{Si}_4$ phase, the average voltages were calculated, indicating that germanium may be a safer alternative to silicon anodes in LIB, due to its higher lithium insertion voltage. Calculations predict high-density Li_1Si_1 and Li_1Ge_1 $P4/mmm$ layered phases which become the ground state above 2.5 and 5 GPa respectively and reveal silicon and germanium's propensity to form dumbbells in the Li_xSi , $x = 2.33 - 3.25$ stoichiometry range. DFT predicts the stability of the $\text{Li}_{11}\text{Ge}_6$ $Cmmm$, $\text{Li}_{12}\text{Ge}_7$ $Pnma$ and Li_7Ge_3 $P32_12$ phases and several new Li-Ge compounds, with stoichiometries Li_5Ge_2 , $\text{Li}_{13}\text{Ge}_5$, Li_8Ge_3 and $\text{Li}_{13}\text{Ge}_4$.

PACS numbers:

I. INTRODUCTION

Lithium-ion batteries (LIBs) are the secondary (rechargeable) battery of choice for portable electronic devices due to their high specific energy (energy per unit weight) and energy density (energy per unit volume). LIBs have the highest capacity of all the commercially available battery technologies and are now being deployed in hybrid and all-electric vehicles.¹ There is substantial interest in enhancing the capacity of LIBs, driven by the economic and environmental advantages of increasing the range of electric vehicles, and enabling longer-life portable electronic devices.

Lithium intercalated graphite is the standard LIB negative electrode material due to its good rate capability and cyclability, but demand for even higher performance LIBs has motivated the investigation of other materials. Silicon is an attractive alternative since it has ten times the gravimetric and volumetric capacity of graphite (calculated from the initial mass and volume of silicon) but, unlike graphite, silicon undergoes structural changes on lithiation.²⁻⁴ The negative electrode may be studied using a half-cell containing lithium and silicon. The term “anode” applies to the negative electrode during LIB discharge only, so to avoid confusion we refer to *lithiation* and *delithiation* of the silicon half-cell which corresponds to charging and discharging the LIB respectively. The first lithiation of the cell at room temperature involves the conversion of crystalline silicon (*c*-Si) into an amorphous lithium silicide phase (*a*- Li_ySi).⁵ The onset of amorphization depends on the lithiation rate and has been measured at

$y \approx 0.3$ in micron-sized (325 mesh) silicon clusters after irreversible SEI (solid-electrolyte interphase) formation has been taken into account.^{6,7} Below a discharge voltage of 50 mV the *a*- Li_ySi crystallizes to form a metastable $\text{Li}_{15}\text{Si}_4$ phase which may become non-stoichiometric, $\text{Li}_{15\pm\delta}\text{Si}_4$, at deep discharge.⁶ However, at temperatures above 100°C it is possible to form the most lithiated crystalline phase, $\text{Li}_{21}\text{Si}_5$, electrochemically.⁸ Full lithiation of silicon leads to a drastic volume expansion of 270–280%,⁹ which generates considerable mechanical stress. Hysteresis in the capacity/voltage profile occurs due to a combination of mechanical stress and different reactions taking different structural pathways on lithiation and delithiation. The microscopic mechanisms underlying these phenomena are still not entirely clear.⁹ *a*- Li_ySi has been studied *in situ* using nuclear magnetic resonance (NMR),⁶ X-ray diffraction (XRD)^{10,11} and electron energy loss spectroscopy (EELS).¹² These studies along with *ex situ* NMR and PDF (pair-distribution function) studies of XRD data suggest that silicon forms small clusters and isolated atoms during lithiation. The clusters that form only break apart into isolated silicon atoms at the end of the lithiation process (below 80 mV).¹³

Many of the disordered structures that form during lithiation can be approximated by the Li-Si ground-state and metastable crystalline phases. For instance, the crystalline phases have been used as a first step in understanding charge transfer¹⁷ and average lithiation voltages.⁴⁵ To gain insight into the possible types of silicon clusters present and their environments in *a*- Li_ySi , various crystalline phases have been investigated and categorized using NMR^{6,14} and *ab initio* theoretical techniques.¹⁵⁻¹⁸ These *c*-Li-Si phases have previously been well categorized using density-functional theory (DFT),¹⁵⁻¹⁷ however new insights into the most lithi-

*Email: ajm255@cam.ac.uk

ated phases and the ability to synthesize Li_1Si_1 through ball milling have suggested that the system is far from fully understood. The most recent phase diagram of the Li-Si system shows, in ascending lithium content order, c -Si, Li_1Si_1 , $\text{Li}_{12}\text{Si}_7$, Li_7Si_3 , $\text{Li}_{13}\text{Si}_4$, $\text{Li}_{15}\text{Si}_4$, $\text{Li}_{22}\text{Si}_5$, and β -Li.¹⁹ Additionally investigations by Zeilinger and coworkers have presented a high-temperature $\text{Li}_{4.11}\text{Si}$ phase^{18,20} and suggested $\text{Li}_{17}\text{Si}_4$ as the correct stoichiometry of $\text{Li}_{21}\text{Si}_5/\text{Li}_{22}\text{Si}_5$.

Germanium is another choice of anode for LIB with a theoretical capacity of 1568 mAh g^{-1} some 5 times greater than carbon. Its lithium diffusivity at room temperature is 400 times greater than silicon,²¹ however it is scarcer and consequently more expensive. About the Li-Ge phase diagram, much less is known. In increasing order of lithium content, the following stable phases have all been proposed: $\text{Li}_7\text{Ge}_{12}$,²² Li_1Ge_1 ,^{23,24} $\text{Li}_{12}\text{Ge}_7$,²² $\text{Li}_{11}\text{Ge}_6$,²⁵ Li_9Ge_4 ,²⁶⁻²⁸ Li_7Ge_3 ,^{22,27} Li_7Ge_2 ,^{28,29} $\text{Li}_{15}\text{Ge}_4$,^{27,28,30,31} $\text{Li}_{17}\text{Ge}_4$ ³² and $\text{Li}_{22}\text{Ge}_5$.^{27,28,33} More crystalline phases occur during electrochemical lithiation of germanium than silicon; XRD and HRTEM measurements show that during lithiation of germanium at room temperature, the Li-Ge system progressed through Li_9Ge_4 , Li_7Ge_2 and a mixture of $\text{Li}_{15}\text{Ge}_4$ and $\text{Li}_{22}\text{Ge}_5$.²⁸

In this article we use atomic species swapping along with random structure searching techniques, described in Sec. II, to predict ground state and metastable crystal structures of the Li-Si and Li-Ge systems. In Sec. III our approach to calculating average voltages is discussed and Secs IV and V describe the DFT-predicted phases of Li-Si and Li-Ge respectively. In the Li-Si system we predict a high-density Li_1Si_1 phase with $P4/mmm$ symmetry and discuss the tendency for silicon to form dumbbells within the lithium silicides. We then turn our attention to Li-Ge which has not been analyzed using these computational search methods method before and predict the new structures, Li_5Ge_2 , $\text{Li}_{13}\text{Ge}_5$, Li_8Ge_3 and $\text{Li}_{13}\text{Ge}_4$. The average voltages for the Li-Si and Li-Ge systems are presented including the $\text{Li}_{17}\text{Si}_4$ and Li_1Si_1 phases. The conclusions of the simulations are given in Sec. VI.

II. METHODS

Ab initio random structure searching (AIRSS) has been successful in predicting the ground-state structures of high-pressure phases of matter.^{34,35} More recently it has also been applied to the Li-P system³⁶ and defects in technologically relevant ceramics,^{37,38} semiconductors^{39,40} and LIBs.^{41,42} Since in an AIRSS calculation each random starting configuration is independent from another, the search algorithm is trivially parallelisable, making high-throughput computation straightforward. AIRSS searches were performed for stoichiometries Li_xSi_y and Li_xGe_y where $x, y = 1 - 8$.

Relaxations were performed using the stoichiometric crystal structures of Li-Si, Li-Ge, Li-Sn, Li-Pb, Na-Si, Na-Ge, Na-Sn, Na-Pb, K-Si, K-Ge, K-Sn and K-Pb. First, the structures were obtained from the International Crystallographic Structure Database (ICSD). Second, for each structure the anions were replaced with Li and the cations replaced with $\{\text{Si, Ge}\}$. The structures were relaxed to local-energy minima

using forces and stresses calculated by DFT.

Calculations were performed using the plane wave CASTEP DFT code.⁴³ The PBE (Perdew-Burke-Ernzerhof) exchange-correlation functional was used with Vanderbilt “ultrasoft” pseudopotentials. The Li-Si system required a basis set containing plane waves with energies of up to 400 eV and a Monkhorst-Pack (MP) grid corresponding to a Brillouin zone (BZ) sampling grid finer than $2\pi \times 0.05 \text{ \AA}^{-1}$. The Li-Ge system required a 600 eV planewave cutoff with harder pseudopotentials and a BZ sampling finer than $2\pi \times 0.03 \text{ \AA}^{-1}$.

We define the formation energy per atom of a compound Li_mX_n , where $X = \{\text{Si, Ge}\}$ as,

$$E_f/A = \frac{E(\text{Li}_n\text{X}_m) - n\mu_{\text{Li}} - m\mu_{\text{X}}}{n+m}, \quad (1)$$

where $E(\text{Li}_n\text{X}_m)$ is the total DFT energy of a given structure, Li_nX_m and μ_{Li} and μ_{X} are the chemical potentials of atomic species Li and X in their ground state elemental structure. To compare the stabilities of different stoichiometries we plot the formation energy per atom, E_f/A versus the fractional concentration of lithium in a compound where,

$$C_{\text{Li}} = \frac{n}{n+m}, \quad (2)$$

and, as above, n and m are the number of atoms of Li and X in a compound respectively. Drawing a convex hull from $(C_{\text{Li}}, E_f/A) = (0, 0)$ to $(1, 0)$, that is, between the chemical potentials, reveals the stable zero Kelvin structures at the vertices of the tie-lines.

III. VOLTAGES

We calculate average voltages in an LIB anode using DFT total energies by assuming that all the displaced charge is due to Li and that the reaction proceeds sequentially through the phases on the tie-lines of the convex hull, *i.e.* it is a succession of two-phase reactions.⁴⁴ The voltage is given by,

$$V = -\frac{\Delta G}{\Delta x}, \quad (3)$$

where the Gibbs free energy change, ΔG is in eV and Δx is the change in the number of lithium atoms per silicon atoms in the 2 phases. The Gibbs free energy is composed of a number of terms,

$$\Delta G = \Delta E + P\Delta V - T\Delta S, \quad (4)$$

where ΔE is the total electronic energy, and P , ΔV , T and ΔS are the pressure, change in volume, thermodynamic temperature and change in entropy respectively. Due to the difficulty in calculating ΔG we make the approximation, previously applied to the Li-Si system, that $\Delta G \approx \Delta E$ since ΔE is of the order of a few electron volts, $P\Delta V \approx 10^{-5} \text{ eV}$ and $T\Delta S \approx 0.06 \text{ eV}$ at 425°C .⁴⁵⁻⁴⁷

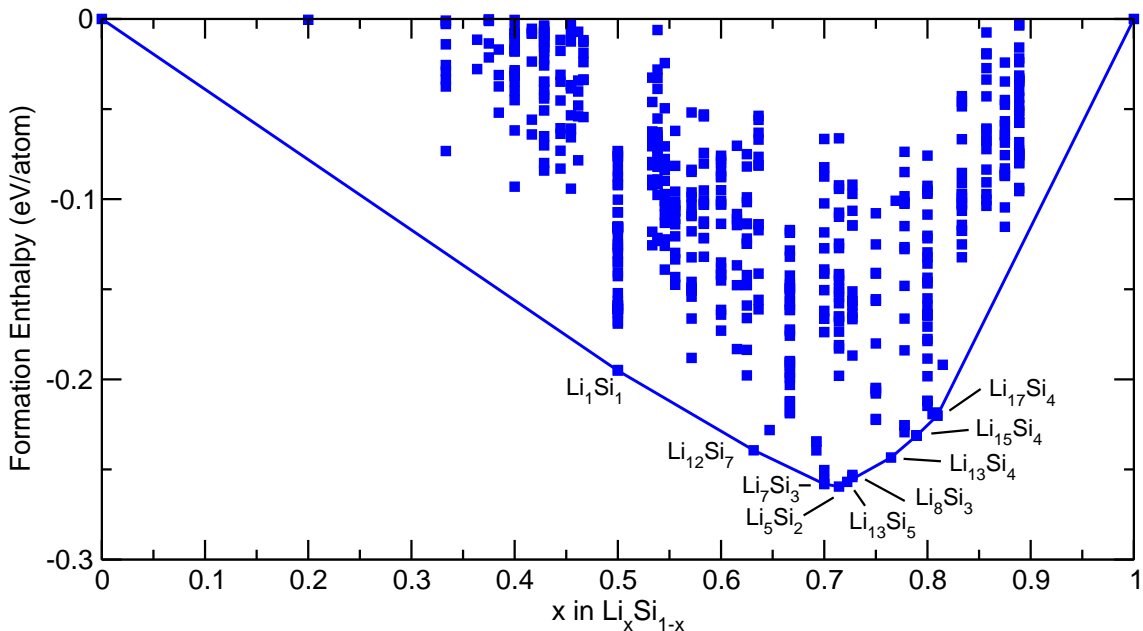


FIG. 1: (Color online) Formation enthalpy per atom versus the fractional lithium concentration of a Li-Si compound (blue boxes). The tie-line (blue line) shows the convex-hull obtained by joining together the globally stable structures predicted by DFT. Between the species swapping technique and AIRSS we recover the known stable phases, Li_1Si_1 , $\text{Li}_{12}\text{Si}_7$, Li_7Si_3 , $\text{Li}_{13}\text{Si}_4$, $\text{Li}_{15}\text{Si}_4$ and $\text{Li}_{17}\text{Si}_4$. The searches also find the Li_5Si_2 phase predicted by Tipton *et al.*⁴⁷ and low-lying metastable phases with stoichiometries Li_8Si_3 and $\text{Li}_{13}\text{Si}_5$ are also predicted.

IV. RESULTS - LITHIUM SILICIDE

We find on the convex hull, shown Fig. 1, in increasing lithium content order; diamond-structure $Fd\bar{3}m$ c -Si; the $I4_1/a$ Li_1Si_1 phase^{48,49} which has recently been synthesized at ambient pressure⁵⁰ and is discussed in Sec. IV A; the $Pnma$ $\text{Li}_{12}\text{Si}_7$ phase⁵¹ which contains silicon 5-membered rings and 4-membered stars, which have been studied using NMR;¹⁴ the Li_7Si_3 and Li_5Si_2 phases with $P3_212$ and $R\bar{3}m$ symmetries respectively discussed further in Sec. IV B; the $Pbam$ $\text{Li}_{13}\text{Si}_4$ phase; the metastable $I4\bar{3}d$ $\text{Li}_{15}\text{Si}_4$; and the $\text{Li}_{17}\text{Si}_4$ $F\bar{4}3m$ symmetry phase discussed further in Sec. IV C.

For $\text{Li}_{15}\text{Si}_4$, Mulikan analysis yields a charge of $0.15|e|$ and $-0.57|e|$ per Li and Si respectively; in agreement with Bader analysis that Li is a cation¹⁷ and contrary to the reports that Li is anionic.⁵²

The average voltage was calculated between all adjacent pairs of stable Li-Si phases on the convex hull including both the $\text{Li}_{17}\text{Si}_4$ phase and Li_1Si_1 phase recently synthesized at ambient pressure. Voltages were obtained from the DFT total energies, as described in Sec. III and referenced to lithium metal. The potential composition curve is presented in Fig 3 as is in agreement with previous experimental and theoretical work.

A. Li_1Si_1 layered structures

We find a set of structures with Li_1Si_1 stoichiometry, listed in Table I, all within ~ 0.1 eV/f.u. of the ground state. The

DFT ground state at 0 GPa is a $I4_1/a$ phase comprising a 3-fold coordinated silicon network hosting lithium tetrahedra similar to the $\{4\text{Li},V\}$ Zintl defect in silicon.⁴² Recently the $I4_1/a$ phase has been synthesized via ball-milling and shown to be stable under ambient conditions.⁵⁰ Mulikan analysis yields a charge of $0.34|e|$ for each Li and $-0.34|e|$ for each Si establishing Li as cationic contrary to a previous analysis.⁴⁹

DFT predicts a novel $P4/mmm$ phase with a formation energy of 0.07 eV p.f.u. at 0 GPa. It is a layered structure comprising a two-dimensional (non-tetrahedrally) four-fold coordinated silicon lattice with lithium intercalated between the silicon sheets. Since the silicon is four-fold coordinated it gains less of the lithium's charge than in the $I4_1/a$ phase; Mulikan analysis shows lithium atoms donate $0.22|e|$ each. Our calculations show the Li_1Si_1 system undergoes a phase transition from the $I4_1/a$ to the $P4/mmm$ phase at 2.5 GPa.

The $I4_1/amd$ phase is isostructural to its Li_1Ge_1 analogue. Li_1Ge_1 $I4_1/amd$ is stable at high pressure,²⁴ however Li_1Si_1 $I4_1/amd$ is not globally stable over the pressure range we studied (between 0 and 10 GPa).

The $P\bar{3}m1$ phase contains 6 membered rings of 3-fold coordinated silicon atoms in layered sheets, see Fig 2. The silicon network is isostructural to silicene, a silicon analogue of graphene. We calculate that silicene and a phase based on the $P4/mmm$ silicon network are 0.63 and 0.89 eV p.f.u. respectively above the $Fd\bar{3}m$ ground state. When lithiated both layered structures are only 0.07 eV above the ($I4_1/a$) ground state. Given the interest in silicene our layered compounds might provide an alternative route to layered silicon.

TABLE I: Low-energy Li_1Si_1 metastable phases. The structures are shown in Fig. 2 with formation energy E_f per formula unit relative to the energy of the ground states. We calculate that $P4/mmm$ is the most stable above 2.5 GPa.

E_f (eV/f.u.)	Symmetry	Volume ($\text{\AA}^3/\text{f.u.}$)	Description
0.00	$I4_1/a$	31.3	Li tetrahedra in a 3-fold coordinated Si network
0.05	$R\bar{3}$	33.1	Distorted Li octahedra 3-fold coordinated Si network
0.07	$P4/mmm$	27.8	Flat Si sheets comprising 4 membered rings
0.07	$P\bar{1}$	31.7	Buckled Si sheets comprising 8 and 4 membered rings
0.07	$P\bar{3}m1$	34.1	Li intercalated silicene
0.08	$P2/m$	28.1	Li_1Sn_1 -like 2.39 \AA dumbbells and isolated atoms
0.11	$I4_1/amd$	28.1	Isostructural with Li_1Ge_1 high-pressure phase

B. Li_7Si_3 and Li_5Si_2

Lithium’s position in the crystal lattice can be difficult to establish due to its low XRD scattering factor. Furthermore, Li_7Si_3 has partially occupied lattice sites⁵³ making it difficult to model using DFT. Its structure may be represented as a supercell of $R\bar{3}m$ Li_5Si_2 in which lithium atoms have been removed from certain lattice sites.⁵⁴ By choosing different combinations of lithium sites in the supercell, models of Li_7Si_3 can be produced with $P\bar{3}m1$, $C2/m$ Cm and $P3_212$ symmetries. The latter, labeled “#2” by Dahn *et al.*,¹⁷ is found on the convex hull.

It is unsurprising that at zero Kelvin, DFT also predicts that the $R\bar{3}m$ Li_5Si_2 phase to be stable since it contains entirely occupied lithium sites. Tipton *et al.* also found this phase to be stable using DFT.⁴⁷

C. Most lithiated phases

The most lithiated stable Li-Si phase has been the subject of debate. XRD measurements predict that $\text{Li}_{21}\text{Si}_5$ ⁵⁵ is stable at room temperature and $\text{Li}_{22}\text{Si}_5$ at 415 $^\circ\text{C}$ ³. Previous DFT calculations predict $\text{Li}_{21}\text{Si}_5$ to be the stabler phase, even after the inclusion of temperature dependence using the harmonic approximation.¹⁷ The combined AIRSS/species-swapping technique predicts $\text{Li}_{21}\text{Si}_5$ and $\text{Li}_{22}\text{Si}_5$ to be locally stable but above the convex hull. The $\text{Li}_{17}\text{Si}_4$ phase is on the convex hull, and it has the same crystal structure as $F\bar{4}3m$ $\text{Li}_{17}\text{Pb}_4$, as discovered independently by Zeilinger *et al.*¹⁸ Zeilinger *et al.* also predict a $\text{Li}_{4.11}\text{Si}$ high-temperature phase which they model using $\text{Li}_{16}\text{Si}_4$ and $\text{Li}_{16.5}\text{Si}_4$ phases. We include Zeilinger *et al.*’s models in Fig. 1 although DFT predicts that they are not on the tie-line.⁷²

D. Repeating units – Silicon dumbbells

We also find a $R\bar{3}m$ Li_8Si_3 and a $P\bar{3}m1$ $\text{Li}_{13}\text{Si}_4$ phase close above the tie-line. They belong to the set of structures in the range $\text{Li}_7\text{Si}_3 \rightarrow \text{Li}_{13}\text{Si}_5$ which all contain silicon dumbbells. The dumbbells are aligned in parallel with various numbers of collinear lithium atoms between them forming one-

TABLE II: Structures in the stoichiometry range Li_xSi , $x = 2.33 - 2.60$ exhibit parallel silicon dumbbells situated in one-dimensional linear columns containing variable numbers silicon dumbbells and isolated lithium and silicon atoms. The columns are packed together realizing the three-dimensional structure. The repeating unit(s) in each column are represented between parentheses, and silicon dumbbells are indicated by Si-Si. For example, a structure comprising columns containing a repeating unit of 5 lithium atoms followed by a silicon dumbbell is represented as $(5 \times \text{Li} + \text{Si-Si})$.

Stoichiometry	Constituent columns
Li_7Si_3	$2 \times (5 \times \text{Li} + \text{Si-Si})$ & $(4 \times \text{Li} + \text{Si-Si})$
Li_5Si_2	$(5 \times \text{Li} + \text{Si-Si})$
$\text{Li}_{13}\text{Si}_5$	$(5 \times \text{Li} + \text{Si})$ & $2 \times (4 \times \text{Li} + \text{Si-Si})$
Li_8Si_3	$(4 \times \text{Li} + \text{Si} + 4 \times \text{Li} + \text{Si-Si})$

dimensional repeating sequences, see Table II. The 1D linear repeating chains are thus packed alongside each other realizing the three-dimensional structure. For example, since Li_7Si_3 comprises $(5 \times \text{Li} + \text{Si-Si})$ and $(4 \times \text{Li} + \text{Si-Si})$ sequences in a ratio of 2:1, it is equivalent to the Li_5Si_2 phase with lithium vacancies. Li_5Si_2 comprises sequences of atoms with the repeating unit $(5 \times \text{Li} + \text{Si-Si})$ and the Li_8Si_3 is similar but with atoms in a $(4 \times \text{Li} + \text{Si} + 4 \times \text{Li} + \text{Si-Si})$ repeating unit; it is isostructural with a Li_8Pb_3 phase.⁵⁶ The $\text{Li}_{13}\text{Si}_5$ phase is isostructural with the $\text{Li}_{13}\text{Sn}_5$ phase⁵⁷ and has two different repeating units $(5 \times \text{Li} + \text{Si})$ and $(4 \times \text{Li} + \text{Si-Si})$ in a ratio of 1:2.

Finally, in $\text{Li}_{13}\text{Si}_4$ the one-dimensional columnar structure does not exist but Si-Si dumbbells and Si isolated atoms remain in a ratio of 1:1. At higher lithium concentrations, $\text{Li}_{15}\text{Si}_4$ forms, in which all silicon dumbbells are broken, and only isolated Si atoms remain. The propensity for silicon dumbbells to form over a wide range of stoichiometries and total energies implies that silicon dumbbells form on lithiation of silicon in a LIB anode.

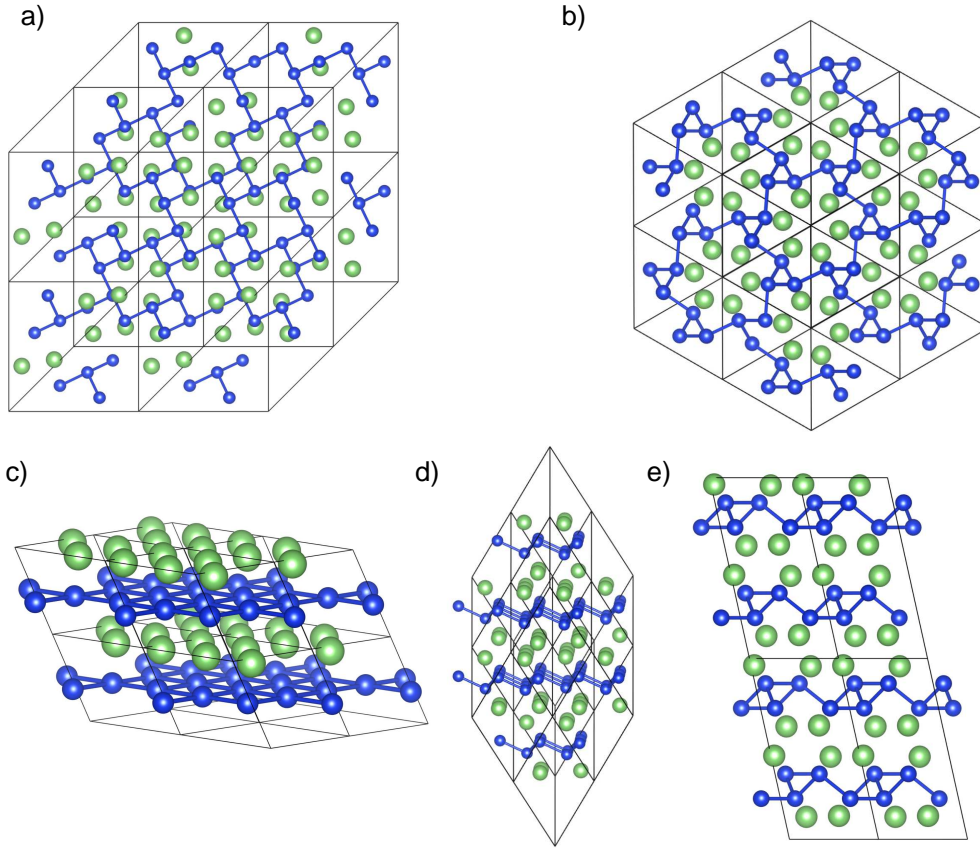
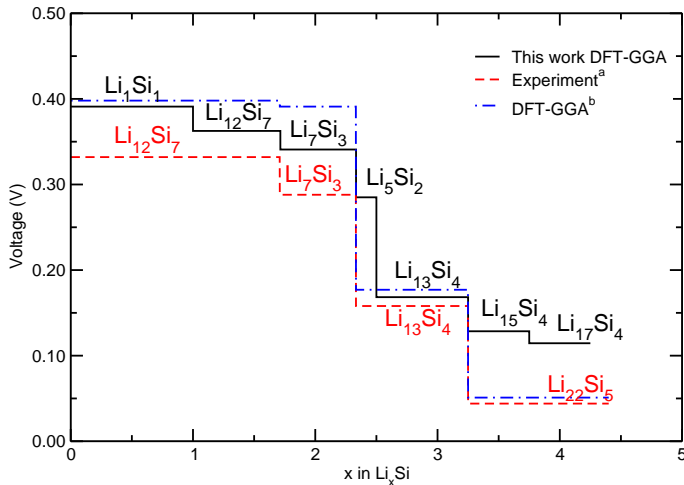


FIG. 2: (Color online) Low-energy Li_1Si_1 phases detailed in Table I with a) $I4_1/a$, b) $R\bar{3}$, c) $P4/mmm$, d) $P\bar{3}m1$, e) $P\bar{1}$ symmetries. DFT predicts the $P4/mmm$ phase to be stable above 2.5 GPa.



^a Wen and Huggins.³

^b Chevrier *et al.*⁴⁵

FIG. 3: (Color online) Potential-composition curves of stable structures found on the convex hull in Fig. 1 (black line) compared to experiment at 415° C (red dashed line) and previous DFT-GGA calculations (blue dot-dashed line).⁴⁵

V. RESULTS - LITHIUM GERMANIDE

In order of lithium content, the following Li-Ge phases have all been proposed: $\text{Li}_7\text{Ge}_{12}$, Li_1Ge_1 , $\text{Li}_{12}\text{Ge}_7$, $\text{Li}_{11}\text{Ge}_6$, Li_9Ge_4 , Li_7Ge_3 , Li_7Ge_2 , $\text{Li}_{15}\text{Ge}_4$, $\text{Li}_{17}\text{Ge}_4$ and $\text{Li}_{22}\text{Ge}_5$. Below we compare in detail the known phases to the results of the DFT searches.

$\text{Li}_7\text{Ge}_{12}$ is the only reported phase with a ratio of Li/Ge less than 1. It has two symmetries associated with it, originally $Pmn2_1$ ^{22,60}, which was later disputed,⁵⁸ and more recently, $P2/n$.⁶¹ Four of its lithium lattice sites are 50% occupied. We model its structure in a periodic lattice using a simulation cell containing 28 Li and 48 Ge sites. The fractionally occupied sites can be filled in a variety of ways: all sites, giving rise to a crystal symmetry $P2/c$: one site ($P1$), four different ways (all degenerate): two sites, 6 ways (Pc , $P2$ or $P\bar{1}$) each symmetry being doubly degenerate): three sites ($P1$) four ways (all degenerate): and by leaving all empty ($P2/c$) one way. A convex hull of their single point energies shows that the (Pc) version is the most stable, hence we use this throughout the rest of the calculations. Although not on the Li-Ge convex hull, see Fig. 4, this Pc predicted phase is close above.

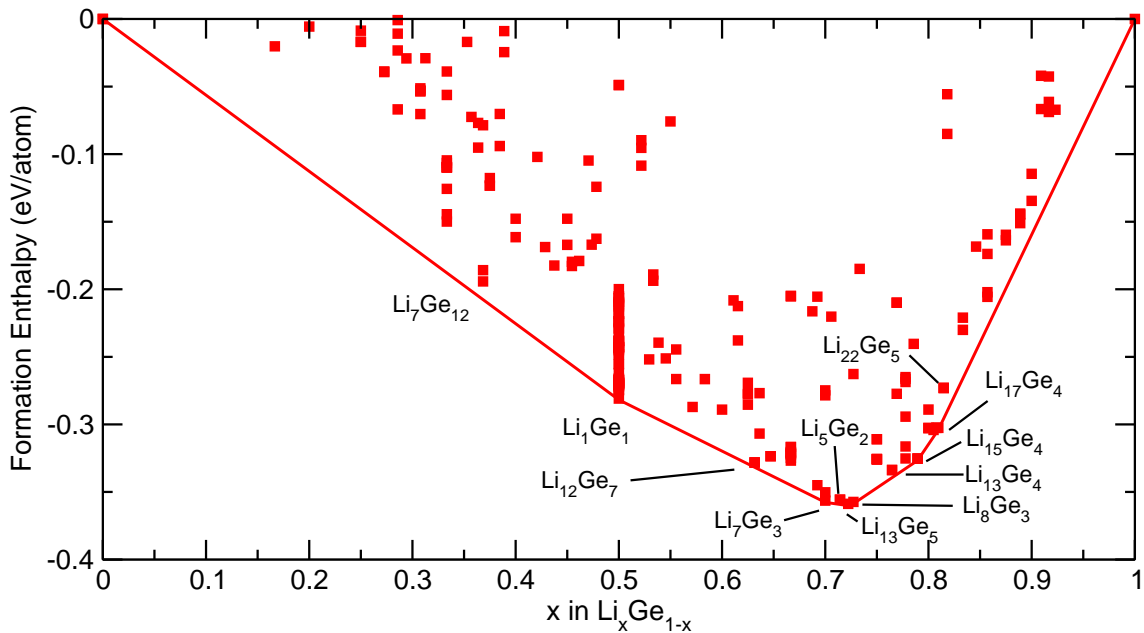


FIG. 4: (Color online) The Li-Ge binary composition diagram. The red squares indicate the formation enthalpy of a structure. The red line is the tie-line indicating the stable structures at 0 K predicted by DFT.

Li_1Ge_1 has an $I4_1/a^{67}$ ground state and a $I4_1/amd^{68}$ high pressure form. DFT predicts $I4_1/amd$ and a new layered $P4/mmm$ phase ~ 0.012 eV/f.u. and ~ 0.020 eV/f.u. above the $I4_1/a$ ground state respectively. The $P4/mmm$ phase is isostructural with the Li-Si phase discussed above in Sec. IV A. DFT predicts that the system undergoes a phase transition from the $I4_1/amd$ to the $P4/mmm$ phase at 5 GPa.

Grüttner *et al.* mentioned a $\text{Li}_{12}\text{Ge}_7$ phase isotypic with the corresponding $\text{Li}_{12}\text{Si}_7$ phase²² in a very brief report, but did not present any further data to support its discovery. DFT also predicts a $\text{Li}_{12}\text{Ge}_7$ $Pnma$ phase near the tie-line.

$\text{Li}_{11}\text{Ge}_6$ was synthesized by Frank *et al.*²⁵ with a molecular volume of $172.3 \text{ cm}^3 \text{ mol}^{-1}$. Nesper *et al.*⁶² claim that the phase is actually Li_8MgGe_6 , suggesting that since Li_8MgGe_6 has a molecular volume of $166.5 \text{ cm}^3 \text{ mol}^{-1}$ it is unlikely that $\text{Li}_{11}\text{Ge}_6$ could have two more atoms per formula unit.⁷³ DFT also finds a $\text{Li}_{11}\text{Ge}_6$ $Cmcm$ phase slightly above the tie-line with a volume of 286.26 \AA^3 per f.u., which corresponds to a molecular volume of $172.4 \text{ cm}^3 \text{ mol}^{-1}$. Hence it seems entirely possible to us that $\text{Li}_{11}\text{Ge}_6$ $Cmcm$ was synthesized by Frank *et al.* as initially proposed.

Li_9Ge_4 in the $Cmcm$ symmetry group, have been made electrochemically and from high temperature fusion,^{27,28,58} but all of our calculations show it well above the tie line, favoring disproportion into a $P32_12$ Li_7Ge_3 phase. Li_7Ge_3 with $P32_12$ symmetry was first mentioned by ref. 22 but no supporting information was given. Jain *et al.* found an unknown phase that they suggested was Li_7Ge_3 fitting the diffraction data to $R\bar{3}m$ symmetry.²⁷ Hence we suggest that Jain *et al.* synthesized either the Li_5Ge_2 or indeed Li_8Ge_3 phases, DFT predicting that both phases have the $R\bar{3}m$ symmetry. Li_5Ge_2 is above the tie-line and $\text{Li}_{13}\text{Ge}_5$ and Li_8Ge_3 are all stable although to the best of our knowledge they have not previously

been presented in the literature. This may be due to thermal effects, see the discussion of similar arguments for Li_5Si_2 in Sec. IV B. $\text{Li}_{16}\text{Ge}_5$ was predicted by St. John, *et al.*⁶⁵ during electrochemical studies. They presented no crystal structure nor is there any prototype structure of $\{\text{Li}/\text{Na}\}\{\text{Si}/\text{Ge}/\text{Sn}/\text{Pb}\}$ with this stoichiometry. DFT predicts a $\text{Li}_{13}\text{Ge}_4$ $Pbam$ phase, isostructural with the $\text{Li}_{13}\text{Si}_4$ phase which is slightly above the tie-line and with a similar Li:Si ratio to $\text{Li}_{16}\text{Ge}_5$. Recently preliminary results by H. Jung *et al.*⁶³ have produced electrochemically new phases in the $\text{Li}_{2.33}\text{Ge} - \text{Li}_{3.5}\text{Ge}$ range whose X-ray pair distribution functions (PDF) match at least one of our predicted phases. A fuller investigation will be presented later.

The Li_7Ge_2 phase with $Cmmm$ symmetry can be made electrochemically and by annealing from high temperature melt.^{28,58} DFT-GGA predicts the $P\bar{3}m1$ phase above the tie-line and 0.08 eV/f.u. more stable than the $Cmmm$ phase. This discrepancy remains after using harder pseudopotentials and either the LDA exchange-correlation or the HSE06 hybrid functional.⁶⁹ A fuller investigation into this will be presented elsewhere.

We find the well known $\text{Li}_{15}\text{Ge}_4$ stoichiometry $I\bar{4}3d$ phase stable.^{27,28,30,31} The most lithiated phase has been a matter of debate in all Li-Group 4 compounds including germanium. Its stoichiometry was reported as $\text{Li}_{22}\text{Ge}_5$ with $F\bar{2}3$ symmetry,³³ due to its similarity to $\text{Li}_{22}\text{Pb}_4$.⁷⁰ More recently, Goward *et al.*³² studied this family of structures and show that for the Ge, Sn and Pb compounds the correct stoichiometry is $\text{Li}_{17}\text{Ge}_4$ with $F\bar{4}3m$ symmetry. $F\bar{4}3m$ symmetry $\text{Li}_{21}\text{Ge}_5$, $\text{Li}_{22}\text{Ge}_5$ and $\text{Li}_{17}\text{Ge}_4$ are found by DFT all at local energy minima. However, $\text{Li}_{17}\text{Ge}_4$ is on the tie-line. Fassler *et al.* also predict a $\text{Li}_{4.10}\text{Ge}$ phase analogous to the $\text{Li}_{4.11}\text{Si}$ phase. We use the same model structures as in the $\text{Li}_{4.11}\text{Si}$ phase for our DFT

TABLE III: Experimental and predicted phases of Li_xGe system.

Experimental Symmetry	x	Stoichiometry	Predicted Symmetry
$Fd\bar{3}m^a$	0.000	Ge	$Fd\bar{3}m$
$Pmn2_1^b, P2/n^c$	0.580	$\text{Li}_7\text{Ge}_{12}$	Pc
$I4_1/a^d, I4_1/amd^{*,e}$	1.000	Li_1Ge_1	$I4_1/a, I4_1/amd^*, P4/mmm^{**}$
$Pnma^f$	1.710	$\text{Li}_{12}\text{Ge}_7$	$Pnma^*$
$Cmcm^g$	1.83	$\text{Li}_{11}\text{Ge}_6$	$Cmcm^*$
$Cmcm^{h,i,j}$	2.25	Li_9Ge_4	$Cmcm^*$
$P32_12^f, R\bar{3}m^i$	2.33	Li_7Ge_3	$P32_12, P21/m^*$
	2.50	Li_5Ge_2	$R\bar{3}m^*$
	2.60	$\text{Li}_{13}\text{Ge}_5$	$P\bar{3}m1$
	2.67	Li_8Ge_3	$R\bar{3}m$
l	3.20	$\text{Li}_{16}\text{Ge}_5$	
	3.25	$\text{Li}_{13}\text{Ge}_4$	$Pbam^*$
$Cmmm^{m,j}$	3.50	Li_7Ge_2	$P\bar{3}m1^*, Cmmm^{**}$
$I\bar{4}3d^{n,i,j}$	3.75	$\text{Li}_{15}\text{Ge}_4$	$I\bar{4}3d$
$F\bar{4}3m^o$	4.20	$\text{Li}_{17}\text{Ge}_4$	$F\bar{4}3m$
$F\bar{4}3m^{p,j,q}$	4.25	$\text{Li}_{22}\text{Ge}_5$	$F\bar{4}3m^*$
$P6_3/mmc^r$	–	αLi	$P6_3/mmc$

Sangster and Pelton's work was invaluable for an overview of the field.⁵⁸

* First metastable above tie-line.

** Second metastable above tie-line.

^a A. W. Hull⁵⁹.

^b Very brief summaries are given by Grüttner *et al.*^{22,60}

^c Kiefer and Fässler.⁶¹

^d E. Menges *et al.*²³

^e J. Evers, *et al.*²⁴

^f Reported in abstract by Grüttner *et al.*²²

^g First found by Frank *et al.*²⁵; Nesper *et al.*⁶² suggested it is actually Li_8MgGe_6 .

^h V. Hopf *et al.*²⁶

ⁱ Jain *et al.*²⁷

^j Yoon *et al.*²⁸

^l E. M. Pell finds Li_3Ge_1 .⁶⁴ See Sangster *et al.*^a and a discussion therein. St. John *et al.* report that they have found the Li_3Ge_1 reported earlier as $\text{Li}_{16}\text{Ge}_5$.⁶⁵

^m V. Hopf *et al.*²⁹

ⁿ Gladyshevskii *et al.*³⁰ and Johnson *et al.*³¹

^o Goward *et al.*³²

^p Gladyshevskii *et al.*³³

^q Reported by Jain *et al.*²⁷ as $\text{Li}_{21.1875}\text{Ge}_5$

^r C. .S. Barrett.⁶⁶

TABLE IV: Low energy Li_1Ge_1 metastable phases, with formation energy, E_f p.f.u relative to that of the energy of the ground state. The structures are isotopic of those found in Li_1Si_1 , as shown in Table I and Fig. 2. DFT predicts that the $P4/mmm$ phase is the most stable above 5 GPa.

E_f (eV/f.u.)	Symmetry	Volume ($\text{\AA}^3/\text{f.u.}$)	Description
0.00	$I4_1/a$	35.1	Li tetrahedra in a 3-fold coordinated Ge network
0.01	$I4_1/amd$	32.2	Known high pressure phase
0.02	$P4/mmm$	31.9	Flat Ge sheets 4 membered rings
0.03	$R\bar{3}$	36.8	Distorted Li octahedra 3-fold coordinated Ge network
0.04	$P2/m$	32.1	Isostructural with the corresponding Li_1Sn_1 phase

calculations. These are above the tie-line as is expected for a high-temperature phase.

The Li-Ge system has an analogous inclination to forming Ge-Ge dumbbells as in Li-Si, as discussed in Sec. IV D.

VI. DISCUSSION

Crystal structures of the Li-Si and Li-Ge systems have been presented, found using both AIRSS searches and atomic species swapping of ICSD structures. Below we discuss the

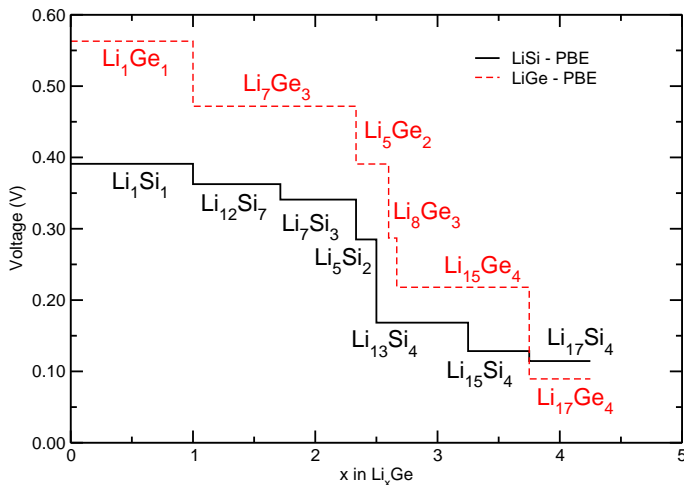


FIG. 5: (Color online) Potential-composition curves of stable structure found on the Li-Si and Li-Ge convex hull diagrams. The Li-Ge results are at a higher average voltage.

structures that are likely to be thermally accessible at room temperature, that is, those at a local minima on the DFT potential energy surface which reside on, or close to, the convex hull. These structures serve as a model for the clustering and bonding behavior of electrochemically lithiated silicon and germanium.⁷¹

The Li-Si system was used to validate our method: DFT finds all of the known phases as local energy minima including independently uncovering the $\text{Li}_{17}\text{Si}_4$ phase. For the Li-Ge system, DFT finds Li_5Ge_2 , Li_8Ge_3 , $\text{Li}_{13}\text{Ge}_5$ and $\text{Li}_{13}\text{Ge}_4$ locally stable and, to the best of our knowledge, these have not been presented in the literature before. DFT predicts that $\text{Li}_7\text{Ge}_{12}$ and $\text{Li}_{11}\text{Ge}_6$ are local energy minima; the former having Pc symmetry and the latter $Cmcm$. It was reported that $\text{Li}_{11}\text{Ge}_6$ may be produced from a high-temperature melt²⁵ but this has been disputed.⁶² Also at local energy minima are the $\text{Li}_{12}\text{Ge}_7$ $Pnma$ and Li_7Ge_3 $P32_12$ phases, which were suggested by Grüttner²² but without presenting the crystal structure. An unknown phase was found by heating ball milled Li-Ge, its XRD pattern fits an Li_7Ge_3 phase with $R\bar{3}m$ symmetry. Since DFT and Grüttner both predict Li_7Ge_3 has $P32_12$ symmetry, we propose that the unknown phase may be either the Li_5Ge_2 or Li_8Ge_3 phases which have a similar stoichiometry to Li_7Ge_3 and both of which DFT predicts to have $R\bar{3}m$ symmetry.

For the Li-Si and Li-Ge structures on the tie-lines, the average voltages were calculated relative to lithium metal. This included for the first time $\text{Li}_{17}\text{Si}_4$ and Li_1Si_1 . The average voltages are in good agreement with both previous calculations and experiment. They are higher in Li-Ge than Li-Si, implying that germanium has a lower energy density than silicon. However the higher insertion voltage is safer during lithiation, reducing the chance of lithium plating which can result in dendrites short circuiting the cell. Lithium in germanium

also has higher diffusivity than in silicon.

Li_1Si_1 was previously only synthesizable at high pressure but has recently been synthesized by highly energetic ball milling, remotivating interest in the high-pressure phases. AIRSS searches predict a selection of higher energy Li_1Si_1 and Li_1Ge_1 phases. At lower pressures three-dimensional three-fold coordinated silicon/germanium networks were prevalent. However, at higher densities, both silicon and germanium exhibited a $P4/mmm$ structure comprising flat sheets of four-fold coordinated silicon and germanium atoms respectively. These became the most stable phase of Li_1Si_1 and Li_1Ge_1 at 2.5 GPa and 5 GPa respectively. Given the interest in silicene our layered compounds might provide an alternative route to layered silicon.

A LIB does not necessarily have time to equilibrate thermodynamically over large length scales.⁶ The ability to generate a wide range of locally-stable low-energy structures above the ground state allows us to visualize the types of clusters which form in the LIB during cycling. Over a lithiation range of Li_xSi , $x = 2.33 - 3.25$ we found that the structures present exhibited Si-Si dumbbells. At higher lithiation all of the silicon dumbbells break up and the crystalline $\text{Li}_{15}\text{Si}_4$ phase forms. Since these dumbbells were seen in both ground state and metastable phases it seems likely that they will exist in LIB anodes, probably in a lower symmetry solid solution. Furthermore we find the analogous dumbbell containing structures in the Li-Ge system.

Above we have demonstrated that the combination of both atomic species swapping the ICSD phases and AIRSS is a powerful tool for predicting the crystal structures of LIB electrode materials. A refinement to the method combines these two techniques by using results of the AIRSS searches as inputs to the species swapping technique. For example, the low-energy structures found by AIRSS in Li_1Si_1 were re-optimized as candidate Li_1Ge_1 phases in the Li-Ge system.

Our method has only provided results of the stable and metastable structures at 0 K, of course, the effect of temperature could be included *post hoc* using phonon calculations within the harmonic approximation and beyond. Our method serves as a crucial first step in *ab initio* materials discovery and design.

Acknowledgments

The authors would like to thank Edgar Engel for useful discussions and Hyeyoung Jung, Yan-Yan Hu and Phoebe K. Allan for sharing their preliminary results and useful discussions. AJM acknowledges the support from the Winton Programme for the Physics of Sustainability. This work was supported by the Engineering and Physical Sciences Research Council (EPSRC) of the U.K. Computational resources were provided by the University College London Research Computing service and the Cambridge High Performance Computing service.

- 1 S. Chu and A. Majumdar, *Nature* **488**, 294 (2012).
- 2 S. Lai, *J. Electrochem. Soc.* **123**, 1196 (1976).
- 3 C. J. Wen and R. A. Huggins, *J. Sol. Stat. Chem.* **37**, 271 (1981).
- 4 W. J. Weydanz, M. Wohlfahrt-Mehrens and R. A. Huggins, *J. Power Sources* **81-82**, 237 (1999).
- 5 J. P. Maranchi, A. F. Hepp and P. N. Kumta, *Electrochem. and Solid-State Lett.* **6**, A198 (2003). P. Limthongkul, Y.-I. Jang, N. J. Dudney and Y.-M. Chiang, *J. Power Sources* **119-121**, 604 (2003). P. Limthongkul, Y.-I. Jang, N. J. Dudney and Y.-M. Chiang, *Acta Mater.* **51**, 1103 (2003).
- 6 B. Key, R. Bhattacharyya, M. Morcrette, V. Seznéc, J.-M. Tarascon, and C. P. Grey, *J. Am. Chem. Soc.* **131**, 9239, (2009).
- 7 J. Li and J. R. Dahn, *J. Electrochem. Soc.* **154**, A156 (2007).
- 8 Kwon, J. H. Ryu and S. M. Oh, *Electrochim. Acta* **55**, 8051, (2010).
- 9 M. N. Obrovac, L. J. Krause, *J. Electrochem. Soc.* **154**, A103 (2007).
- 10 T. D. Hatchard and J. R. Dahn, *J. Electrochem. Soc.* **151**, A838 (2004).
- 11 M. N. Obrovac and L. Christensen, *Electrochem. and Solid-State Lett.* **7**, A93 (2004).
- 12 Y.-M. Kang, S.-B. Suh, and Y.-S. Kim, *Inorg. Chem.* **48**, 11631 (2009).
- 13 B. Key, M. Morcrette, J.-M. Tarascon, and C. P. Grey, *J. Am. Chem. Soc.* **133**, 503, (2011).
- 14 T. K.-J. Köster, E. Salager, A. J. Morris, B. Key, V. Seznec, M. Morcrette, C. J. Pickard and C. P. Grey, *Angew. Chem. Int. Ed.* **123**, 12799 (2011).
- 15 V. L. Chevrier and J. R. Dahn, *J. Electrochem. Soc.* **157**, A392-A398 (2010).
- 16 V. L. Chevrier and J. R. Dahn, *J. Electrochem. Soc.* **156**, A454-A458 (2009).
- 17 V. L. Chevrier, J. Zwanziger and J. R. Dahn, *J. Alloy Compd.* **496**, 25-36 (2010).
- 18 M. Zeilinger, I. M. Kurylyshyn, U. Häussermann and T. F. Fässler, *Chem. Mater.* **25**, 1960 (2013).
- 19 H. Okamoto, *J. Phase Equilib. Diffus.* **30**, 118, (2009).
- 20 M. Zeilinger, I. M. Kurylyshyn, U. Häussermann and T. F. Fässler, *Chem. Mater.* 2013 published online (dx.doi.org/10.1021/cm4029885).
- 21 C.-M. Park and J.-H. Kim and H. Kim and H.-J. Sohn, **39** 3115, (2010). *Chem. Soc. Rev.*
- 22 A. Grüttner, R. Nesper, and H. G. von Schnering, *Acta Crystallog. A* **37**, Supl. C161 (1981).
- 23 E. Menges, V. Hopf, H. Schäfer and A. Weiss, *Z. Naturforsch B*, **24**, 1351, (1969).
- 24 J. Evers, G. Oehlinger, G. SEXTL and H.-O. Becker, *Angew. Chem. Int. Ed.* **26** 76, (1987).
- 25 U. Frank and W. Müller *Z. Naturforsch. B*, **30B**, 313, (1975).
- 26 V. Hopf, H. Schäfer and A. Weiss, *Z. Naturforsch B*, **25**, 653, (1970).
- 27 A. Jain, E. Kawasako, H. Miyaoka, T. Ma, S. Isobe, T. Ichikawa and Y. Kojima, *J. Phys. Chem. C* **117**, 5650 (2013).
- 28 S. Yoon, C.-M. Park, and H.-J. Sohn, *Electrochem. and Sol. Stat. Lett.* **11**, A42 (2008).
- 29 V. Hopf, W. Müller and H. Schäfer, *Z. Naturforsch B*, **27**, 1157, (1972).
- 30 E. L. Gladyshevskii and P. I. Kripyakevich, *Sov. Phys.-Cryst.*, **5**, 549 (1961).
- 31 Q. Johnson, G. S. Smith and D. Wood, *Acta Cryst.* **18**, 131, (1965).
- 32 G. R. Goward, N. J. Taylor, D. C. S. Souza and L. F. Nazar, *J. Alloy Comp* **329**, 1-2, 82, (2001)
- 33 E. L. Gladyshevskii, G. I. Oleksiv and P. I. Kripyakevich, *Sov. Phys.-Cryst.*, **9**, 269 (1964).
- 34 C. J. Pickard and R. J. Needs, *Phys. Rev. Lett.* **97**, 045504 (2006).
- 35 C. J. Pickard and R. J. Needs, *J. Phys.: Condens. Matter* **23**, 053201 (2011).
- 36 A. S. Ivanov, A. J. Morris, K. V. Bozhenko, C. J. Pickard and A. I. Boldyrev, *Angew. Chem. Int. Ed.* **51**, 8330 (2012).
- 37 J. Mulroue, A. J. Morris, and D. M. Duffy, *Phys. Rev. B*, **84**, 094118 (2011).
- 38 J. Mulroue, M. Watkins, A. J. Morris, and D. Duffy, *J. Nucl. Mat.* **437**, 1-3, 261 (2013).
- 39 A. J. Morris, C. J. Pickard and R. J. Needs, *Phys. Rev. B* **78**, 184102 (2008).
- 40 A. J. Morris, C. J. Pickard and R. J. Needs, *Phys. Rev. B* **80**, 144112 (2009).
- 41 A. J. Morris, C. P. Grey, R. J. Needs and C. J. Pickard, *Phys. Rev. B* **84**, 224106 (2011).
- 42 A. J. Morris, R. J. Needs, E. Salager, C. P. Grey and C. J. Pickard, *Phys. Rev. B* **87**, 174108, (2013).
- 43 S. J. Clark *et al.*, *Z. Kristallogr.* **220**, 567 (2005).
- 44 M. K. Aydinol, A. F. Kohan, G. Ceder, K. Cho and J. Joannopoulos, *Phys. Rev. B*, **56**, 1354, (1997).
- 45 V. L. Chevrier, J. W. Zwanziger and J. R. Dahn, *Can. J. Phys.* **87**, 625, (2009).
- 46 I. A. Courtney, J. S. Tse, O. Mao, J. Hafner and J. R. Dahn, *Phys. Rev. B*, **58**, 15583 (1998).
- 47 W. W. Tipton, C. R. Bealing, K. Mathew and R. G. Hennig, *Phys. Rev. B*, **87**, 184114 (2013).
- 48 L. A. Stearns, J. Gryko, J. Diefenbacher, G. K. Ramachandran, and P. F. McMillan, *J. Sol. Stat. Chem.* **173**, 251, (2003).
- 49 Y. Kubota, M. C. S. Escaño, H. Nakanishi and H. Kasai, *J. Alloys Comp.* **458** 151 (2008).
- 50 Wan Si Tang, Jean-Noël Chotard and Raphaël Janot, *J. Electrochem. Soc.* **160** A1232 (2013).
- 51 R. Nesper, H. G. von Schnering and J. Curda, *Chem. Ber.* **119**, 3576 (1986).
- 52 Y. Kubota, M. C. S. Escaño, H. Nakanishi and H. Kasai, *J. App. Phys.* **102** 053704, (2007).
- 53 H.-G. von Schnering, R. Nesper, K.-F. Tebbe and J. Curda, *Z. Metallkde.* **71**, 357, (1980).
- 54 I. Barvík, *Czech. J. Phys. B* **33** (1983).
- 55 R. Nesper and H. G. von Schnering, *J. Sol. Stat. Chem* **70**, 48, (1987).
- 56 K. Cenzual, M. N. Gelato, M. Penzo and E. Parthe, *Z. Kristallog.* **193**, 217, (1990).
- 57 U. Frank and W. Müller, *Z. Naturforsch. B.* **30**, 316, (1975).
- 58 J. Sangster and A. D. Pelton, *J. Phase Equilib.* **18** 289 (1997).
- 59 A. W. Hull, *Phys. Rev.* **20**, (Minutes of the Washington Meeting), 113, (1922).
- 60 A. Grüttner, R. Nesper, and H. G. von Schnering, *Agnew. Chem. Int. Ed.* **21**, 12, 912 (1982).
- 61 F. Kiefer and T. F. Fässler *Sol. State. Sci.* **13**, 636, (2011).
- 62 R. Nesper, J. Curda and H. G. von Schnering, *J. Sol. Stat. Chem.* **62**, 199, (1986).
- 63 H. Jung, Y.-Y. Yau, P. K. Allen and C. P. Grey.
- 64 E. M. Pell, *J. Phys. Chem. Solids* **3**, 74, (1957).
- 65 M. R. St. John, A. J. Furgala and A. F. Sammells, *J. Electrochem. Soc.* **129**, 247, (1982).
- 66 C. S. Barret, *Phys. Rev.* **72** 245, (1947)

- ⁶⁷ E. Menges, V. Hopf, H. Schaefer and A. Weiss, *Z. Natur. B* **27**, 313, (1975).
- ⁶⁸ J. Evers, G. Oehlinger, G. SEXTL and H. O. Becker, *Angew. Chem. (Ger. Ed)* **99**, 69, (1987).
- ⁶⁹ A. V. Krukau, O. A. Vydrov, A. F. Izmaylov and G. E. Scuseria, *J. Chem. Phys.* **125**, 224106 (2006)
- ⁷⁰ A. Zalkin and W. J. Ramsey, *J. Phys. Chem.* **62**, 689, (1958).
- ⁷¹ K. Ogata, E. Salager, C. J. Kerr, A. E. Fraser, C. Ducati, A. J. Morris, S. Hofmann and C. P. Grey *Nature Comm.* **5**, 3217, (2014).
- ⁷² Since the $\text{Li}_{16.5}\text{Si}_4$ model contains partially occupied Li sites we extended the cell in the *a* direction fully occupying four 8g and two 4c sites before optimizing the geometry using DFT.
- ⁷³ Confusingly Sangster and Pelton⁵⁸ report that Nesper *et al.* claim it is the Li_8MgSi_6 phase.